

# FUSION OF REMOTELY SENSED MULTISPECTRAL IMAGERY AND LIDAR DATA FOR FOREST STRUCTURE ASSESSMENT AT THE TREE LEVEL

S. S. Ali<sup>a,\*</sup>, P. Dare<sup>b</sup>, S. D. Jones<sup>c</sup>

<sup>a,b</sup> School of Geography, Population and Environmental Management, Flinders University, Adelaide, South Australia  
- (sohel.syed, paul.dare)@flinders.edu.au

<sup>c</sup> Mathematical & Geospatial Sciences, RMIT University, Melbourne - simon.jones@rmit.edu.au

## Commission VII, WG VII/6

**KEY WORDS:** Airborne remote sensing, Classification, Digital photogrammetry, Fusion, Forestry, Lidar, Multispectral imagery

### ABSTRACT:

A new feature-level fusion is presented for modelling individual trees by applying watershed segmentation and subsequent classification, using tree heights and tree crown signatures derived from light detection and ranging (lidar) data and multispectral imagery. The study area is part of the Moira State Forest, New South Wales, Australia where the dominant tree species are native eucalypts. In this study, airborne lidar data and four band multispectral imagery were acquired. A digital surface model (DSM) was generated from the lidar first return data and a digital terrain model (DTM) was derived from the lidar last return data. A tree crown model was computed as the difference between DSM and DTM using appropriate height thresholds. A marker-controlled watershed segmentation algorithm was used to extract individual tree crowns from the lidar data. The resulting crown polygons were overlaid on the four band multispectral imagery to extract the spectral signatures of the tree crowns. A principal components transformation was applied to the four-band dataset to replace the highly correlated original bands with those of reduced correlation. In addition, two lidar derived texture and height layers were included in the fusion procedure. The application of the maximum likelihood technique led to a high classification accuracy. An average classification accuracy of 86 percent was achieved and this procedure outperformed the original four-band maximum likelihood classification by 23 percent. The success of the tree crown extraction algorithm in old growth areas was higher than in more juvenile areas where the crowns were more scattered. It was also observed that large crowns were better delineated than small ones. The results indicate that this fusion modelling strategy may prove suitable for estimating and mapping the crown area, height and species of each tree.

## 1. INTRODUCTION

### 1.1 Motivation

Individual tree components (both in the horizontal and vertical plane) are important parameters for developing a better understanding of how forest ecosystems function. Lidar data provide accurate measurements of forest structure in the vertical plane; however, current lidar sensors have limited coverage in the horizontal plane. Conversely, high resolution multispectral imagery provides extensive coverage of forest structure in the horizontal plane, but is relatively insensitive to variation in the vertical plane. Therefore, it is desirable to synergistically use both sensors for mapping forest parameters at a fine scale. Delineating individual trees and extracting relevant tree structure information from fused remotely sensed data have significant implications in a variety of applications such as reducing fieldwork required for forest inventory (Gong *et al.*, 1999), assessing forest damage (Kelly *et al.*, 2004) and monitoring forest regeneration (Clark *et al.*, 2004).

### 1.2 Imagery and lidar data fusion

There have been several attempts to fuse lidar and high spatial resolution imagery for individual tree attributes collection (Baltsavias, 1999; Leckie *et al.*, 2003). The strong argument of fusion is that the lidar measurements do not distribute homogeneously and usually have gaps between them. As a

result, the three-dimensional structure of the objects might not be very well defined (Baltsavias, 1999). It thus becomes fairly complex to obtain a good 3D model of the canopy architecture of each tree with a low density of lidar returns. The idea of exploiting the complementary properties of lidar and aerial imagery is to extract semantically meaningful information from the aggregated data for more complete surface description. Sua'reza *et al.* (2005) propose a data fusion analysis with lidar and aerial photography to estimate individual tree heights in forest stands. The tree canopy model is derived from lidar layers as the difference between the first pulse and last pulse return. Information about individual trees was obtained by object-oriented image segmentation and classification. This analysis provided a good method of estimating tree canopies and heights. However, the method of segmentation and classification are too image dependent. The classification parameters were not defined automatically and exhibit no clear relationship to allometry factor. Instead, they were defined empirically following a trial-error process. Leckie *et al.* (2003) applied the valley following approach in to both lidar and multispectral imagery and found that the lidar can easily eliminate most of the commission errors that occur in the open stands while the optical imagery performs better for isolating trees in Douglas-fir plots.

This study attempts to use a new feature-level fusion methodology for modelling individual trees. The method

\* Corresponding author.

incorporates the watershed segmentation algorithm and subsequent classification using tree heights and tree crown signatures derived from both lidar data and multispectral imagery.

## 2. STUDY AREA AND DATASETS

The study area is part of the Moira State Forest, New South Wales, Australia where the dominant tree species are native eucalypts. River Red Gum (*Eucalyptus camaldulensis ssp. obtusa* Dehnh), Black Box (*Eucalyptus largiflorens*), and Grey Box (*Eucalyptus microcarpa*) are common tree species found in the Moira State Forest.

### 2.1 Lidar data

The lidar data used for this project was acquired by AAMGeoScan (now AAMHatch) in May, 2001. The lidar system used was the ALTM 1225, which operates with a sampling intensity of 11000 Hz at a wavelength of 1.047  $\mu\text{m}$ . The approximate flying height of this sensor was 1100m and the laser swath width was 800m. Vertical accuracy was 0.15m ( $1\sigma$ ), the internal precision was 0.05m, and the original laser footprint was 22cm in diameter. The original lidar dataset was processed by AAMHatch and provided to the Victorian Department of Sustainability and Environment (DSE). The provided data were two separate files representing the first and last return point clouds. The original lidar data had point spacing in the order of 16 points per  $\text{m}^2$  and was resampled to a 1m grid.

### 2.2 Multi-spectral imagery

The multi-spectral imagery was captured over the study area using an Ultracam-D with a calibrated focal length of 101.400mm. Three colour (red, green and blue) and one infrared (IR) band images were collected with a 28.125 $\mu\text{m}$  pixel size. The radiometric resolution of the images was 16-bit. This increased radiometric range captures more detailed information of the land cover features. As a result, in extreme bright and dark areas we still manage to get redundant information, which is beyond what is visible in images with lower radiometric resolution (Leberl and Gruber, 2005).

## 3. METHODOLOGY

The proposed scheme includes five parts: (1) data pre-processing, (2) watershed segmentation, (3) data processing, (4) supervised classification and (5) accuracy assessment. The flowchart in Figure 1, illustrates the major steps, which are performed through this data fusion project.

### 3.1 Data pre-processing

The data pre-processing stage consists of two major steps: (1) normalised digital surface model (nDSM) generation from lidar data and (2) geometric correction of multispectral imagery. The lidar first and last return height data were used to generate the nDSM for the tree crowns. The last return of the lidar normally represents the digital terrain model (DTM) and the first return as the digital surface model (DSM). A height difference between the DSM and DTM represents the absolute height of the trees. A height threshold was applied to remove low-lying vegetation (<1.5m) close to the terrain surface. This nDSM

along with lidar 1<sup>st</sup> return intensity and multispectral images was used in the data fusion process.

Using the exterior orientation parameters (X, Y, Z,  $\omega$ ,  $\phi$ ,  $\kappa$ ) derived from onboard GPS and INS sensors and ground control points the geometric correction of the multispectral imagery was accomplished. The exterior orientation parameters for each aerial photograph were supplied with the camera calibration certificate, which were used for the orthorectification of the aerial photographs. An optimal number of ground control points were derived using differential GPS to increase the geometric corrections of the multispectral imagery.

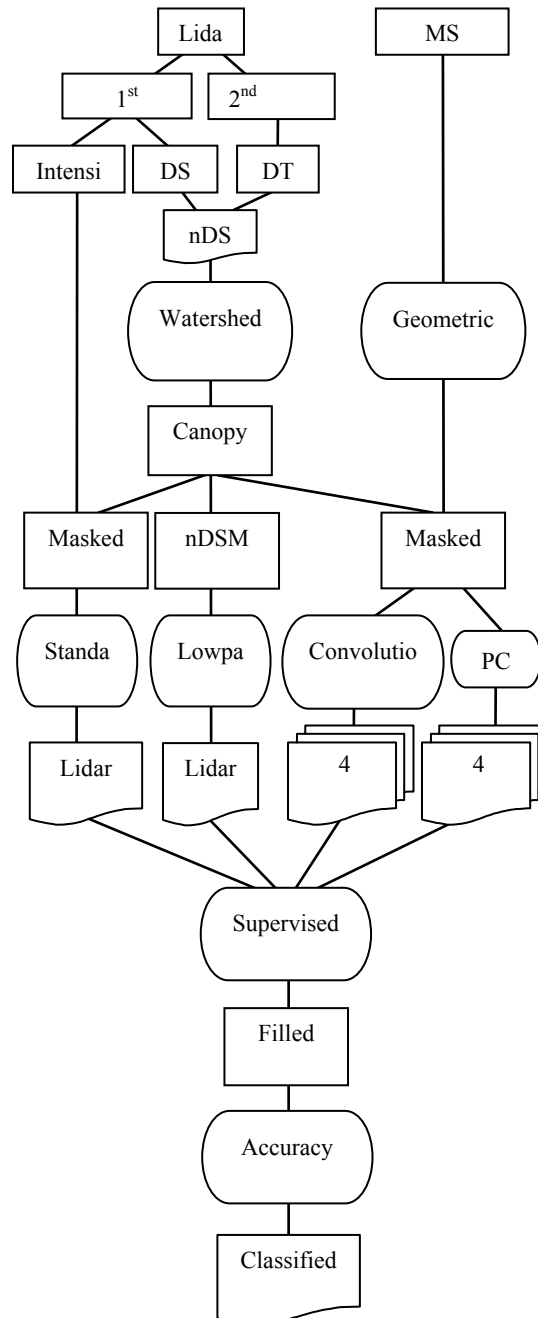


Figure 1. Flowchart of tree type classification using lidar and multispectral imagery.

Some temporal effects were expected in the data fusion process, due to the differences in acquisition time of the lidar (in 2001)

and the multispectral imagery (in 2004). These were the only available images for this research project; therefore we had to compromise on this issue. The study area is a slow growing forest and within this time frame it had not seen any abrupt changes such as tree damage by bush fire or logging. However, some temporal effects were found, due mainly to the natural growth of trees, which is always a challenge to address in high resolution data fusion.

### 3.2 Watershed segmentation

The lidar derived nDSM represents the tree canopies of the forest. Single and disjoint tree canopies can easily be delineated in this process. However, a segmentation procedure is needed to isolate trees which are grouped. This study uses marker-controlled watershed segmentation for tree canopy isolation. Watershed segmentation, first proposed by Beucher and Lantuejoul (1979), is a well known image segmentation method that incorporates region growing and edge detection techniques (Soille,2003). To avoid the over segmentation problem, Meyer and Beucher (1990) introduced marker-controlled watershed segmentation. The idea is to perform watershed segmentation around user-specific markers rather than the local maxima in the input image.

In the watershed segmentation of the nDSM data, the tree crown model was treated as a 3D surface, with lateral dimensions representing the image plane, and the vertical dimension representing the grey values (Figure 2a). Internal markers were used to locate the local minima, which were associated with high grey values (i.e. selected tree crowns) and external markers were pointed to the local maxima, which were associated with the background. Through flooding from the local minima, the watershed segmentation was performed: neighbouring watersheds were merged unless boundaries were built to isolate individual tree features (Figure 2c). The process of merging regions and building boundaries continued until no more region growing could take place.

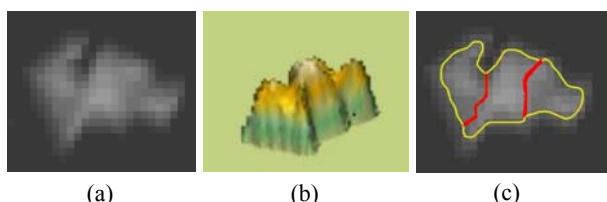


Figure 2. An illustration of watershed segmentation. (a) A canopy model derived from nDSM, (b) 3D view of the canopies, and (c) Segmentation results with dams (in red) built at the divide line.

### 3.3 Data processing

After segmentation, the resulting crown polygons were overlaid on the lidar and multispectral imagery to extract the spectral signatures and texture information of the tree crowns for tree species discrimination. Firstly, the extracted signatures from four of the original multispectral bands were processed with a directional convolution filter using a 3x3 window. This filtering procedure allowed the suppression of shadow effects within the sunlit area of the tree crown. The weighting factors and the dimensionality of the filter are primarily dependent on the solar direction at the time of over flight, the tree size, and the illumination conditions within the tree crown.

Secondly, image enhancement by principal components transformation was applied to the filtered four-band data set. The objective being the replacement of the highly correlated original bands with those of reduced correlation. The transformation resulted in four new components: the brightness, the redness, the greenness, and the blue-yellowness, for each of the tree types.

In addition, two more lidar derived layers were included in the fusion procure. A ninth layer was generated by a texture analysis of the first return lidar intensity and the tenth layer from lidar derived nDSM layer.

### 3.4 Supervised classification

A supervised classification of the 10 layer datasets into three different categories as listed in Table 1 was carried out. Much of the success of the maximum likelihood classifiers depends on the choice of training areas. Extensive field survey measurements were conducted to collect the training data. The processed datasets were also used to redefine the training area in order to maximize the classification results. These datasets allowed a much better class-specific delineation of the training areas involving a reduced sample size for the different tree categories. However, the selected training areas still met the minimal requirement of  $5 \times k$  (no. of layers) pixels from a statistical point of view (Kalayeh and Landgrebe,1983).

Class	Tree type	Description
1	Black Box	Rough bark
2	Grey Box	Fine, pale, fibrous bark
3	River Red Gums	Smooth bark

Table 1. Selected tree classes and associated degree of disease

**3.4.1 Filling the tree polygon:** In high spatial resolution data fusion, the class variability within tree crown is caused mainly by the variability in crown structure (shadow effects), crown density (background material) and different tree components (bark, needles/leaves) (see figure 3a). In addition, the class variability is also affected by the categorisation of the tree types with respect to the leave and bark patterns (Table 1).

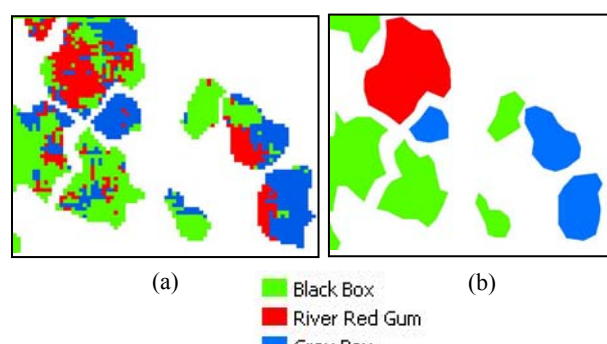


Figure 3. Refining the tree classification; (a) the classified tree crowns; (b) Filling the tree crown area with majority species.

In order to increase the significance of the classification results, the entire tree polygon was filled with the most frequent class (Figure 3a). In this way, only one class occupied the entire

polygon despite the classification of only a fraction of a tree crown (Figure 3b).

### 3.5 Accuracy assessment

To evaluate accuracy, ground truth tree types and crown maps for six plots (Appendix A), each with an area of 50m by 50m, were acquired in the field. Existing aerial photography was used to design the sample plots and tree information was collected by the field survey. There are a total of 61 trees in the six plots. An error matrix was generated from the field sample data corresponding to the fused results.

## 4. RESULTS AND DISCUSSION

Figure 4 illustrates the close correspondence ( $r^2 = 0.87$ , 95% Confidence level, standard error = 0.67m) between tree mean heights derived from both field measurements and lidar data was observed. The comparison suggested, however, that the mean height was more reliably estimated for trees with large and relatively flat crown areas than those were small and pointed crowns.

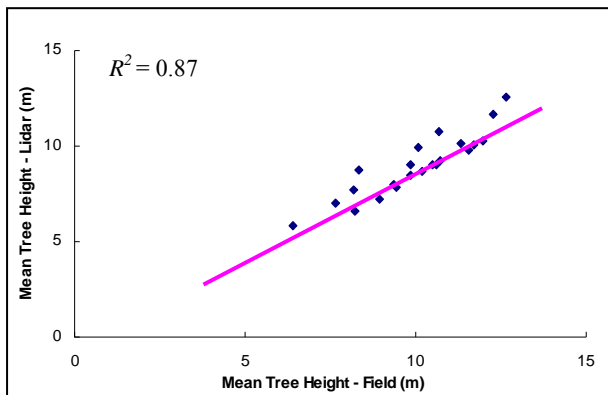


Figure 4. Relationship between individual tree mean heights as estimated in the field and from lidar.

Results from previous studies have shown that isolating deciduous tree species in lidar data is difficult due to their complex structure (Chen *et al.*, 2006). However, the use of the marker-controlled watershed segmentation algorithm with the lidar data achieved a satisfactory result for eucalypt trees. The success of the tree crown extraction algorithm in old growth areas was higher than in more juvenile areas where the crowns are more scattered. It was also observed that large crowns were better delineated than small ones.

To study the correlation between tree height and crown size, tree height and crown size were measured from the crown segments. Crown size is the average crown diameter and was derived from the shape file generated area and algorithm for the relationship of the crown area and radius. From the tabular dataset, the trees were randomly sampled over the whole study area and the sample size was 100 trees. It was found that crown size has larger variability when a tree height is higher, which will contradict the assumption of homoscedasticity if a linear model is fitted. To avoid this issue, a parameterised non-linear model was fitted:

$$\text{CrownSize} = 12.080 - 25.43e^{-0.1906(\text{TreeHeight})} \quad (1)$$

Using Equation (1) a fitted line was generated through the scatter plot as illustrated in Figure 5. In the regression analysis, the relationship between crown size and tree height followed a non-linear curve and mean squared error is 0.52, implied a low level correlation.

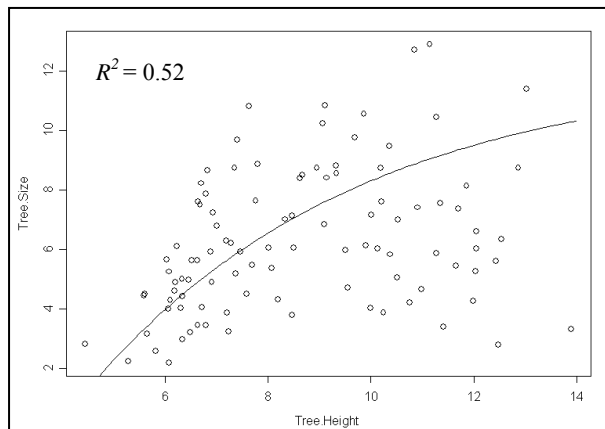


Figure 5. The relationship between crown size and tree height.

The application of the maximum likelihood classification technique involving the original four-band data set led to low classification accuracy. The main reason was the confusion within classes due to the noise effects such as shadows, background vegetation and lack of information. An improvement of the classification was achieved with the integration of lidar derived height and intensity data. Additionally, eight new layers generated from multispectral data substantially reduced interclass confusion compared to the original four-band data. The class separability was also improved for particular tree species by increasing the gap between the class means and reducing the class variability. The use of the tree polygons derived from watershed segmentation markedly improved the classification results through the assignment of the most frequent pixel to the particular tree polygon as shown in Figure 3b. In this way, only one class occupied the entire polygon despite the classification of only a fraction of a tree crown.

The results of the accuracy assessment are summarised in Table 2. The accuracy was assessed by comparing the classified tree crown with the true tree information derived from field survey. An average classification accuracy of 86 percent was achieved and this procedure outperformed on average the original four-band maximum likelihood classification by 23 percent. The separation between the classes Black Box and Grey Box was improved with the fused 10 layer datasets. This is mainly due to the incorporation of the lidar data and the four principal components of the multispectral imagery, into the classification.

Classification types	Classification accuracy (%)
Only multi spectral (4 layer)	63
Fused multi spectral and lidar data (10 layer)	86

Table 2 Comparative accuracy assessments.

The classification accuracies achieved are comparable to those produced by visual interpretation. Map scatter plots of lidar return combined with multispectral imagery and field data enabled, in some cases, visual discrimination at the individual tree level between Black Box and Grey Box. While a clear distinction between these two species was not always visually obvious at the individual tree level, due to other extraneous sources of variation in the dataset, the observation was supported in general at the site level. Sites dominated by Black Box generally exhibited a lower proportion of singular lidar returns compared to sites dominated by Grey Box. River Red Gums can easily be distinguished from others by their unique spatial distribution. This species is largely populated throughout the forest surrounding the Riverine wetlands that are subject to periodic inundation (see Appendix A).

The fusion procedure proposed in this study demonstrates the usefulness of the five main processing steps to cope with the classification of very high spatial resolution lidar and multispectral imagery. This approach can be used in principle for species classification of high spatial resolution data. However, sensor-specific modifications to these different processing steps have to be made in order to maximise the fusion results.

## 5. CONCLUSIONS

The investigation presented in this paper has been conducted to establish an automated procedure for forest species identification at the tree level from high spatial resolution imagery and lidar data. For this purpose, four-band multispectral imagery and lidar data were used to develop a feature-level fusion approach. This technique consists of five steps: the preprocessing of the lidar and multispectral data; tree crown polygon extraction using marker-control watershed segmentation; masking of spectral, height and textural information using the crown polygons; classification of the polygon data; and, the accuracy assessment.

In contrast to the original four-band multispectral data sets, the average classification accuracy was considerably improved through the generation of additional features using the principal component transformation, filtering techniques, and texture analysis. Principal component transformation of the multispectral imagery added more layers to separate different tree species. The addition of the height and texture features derived from lidar data resulted in an improved discrimination of the tree classes.

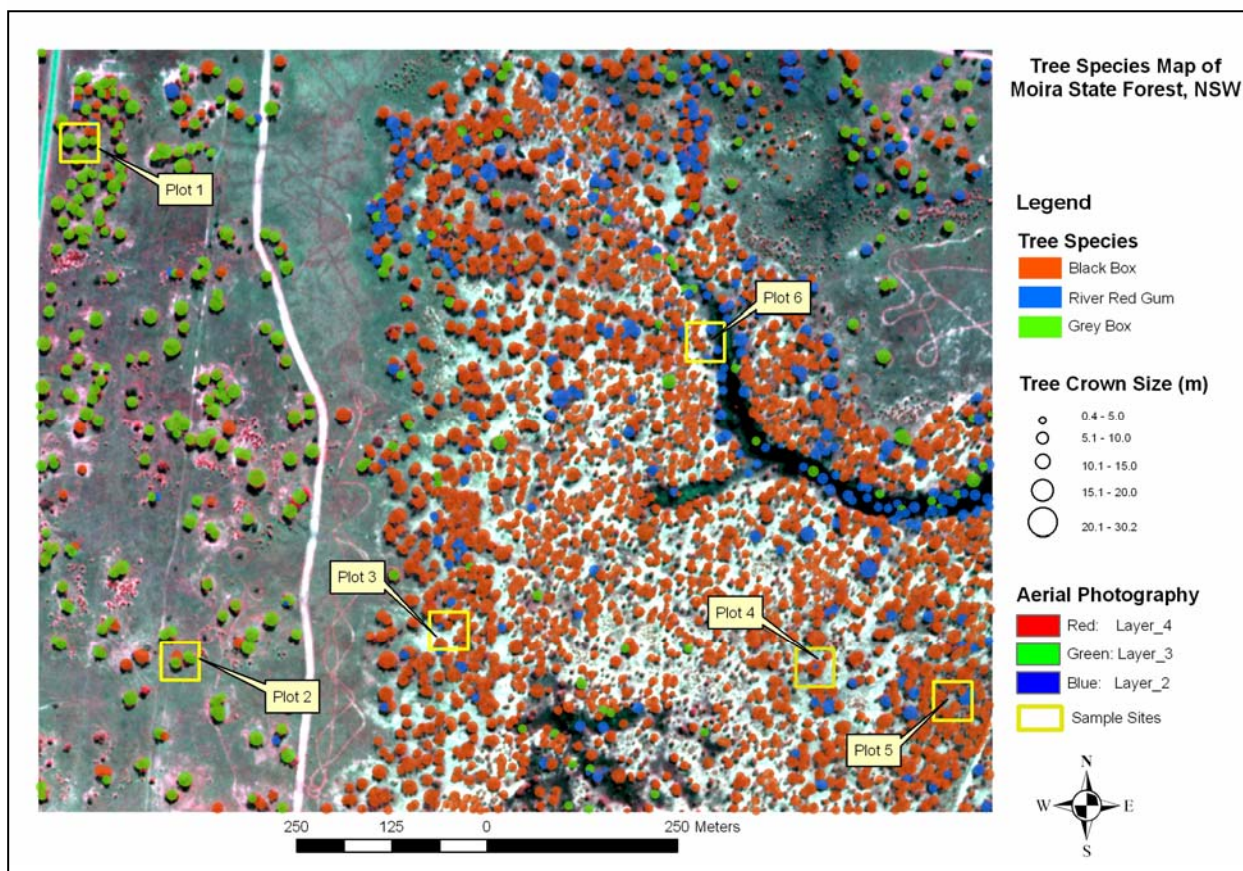
The superposition of the watershed derived crown polygon on to the images was essential for achieving good classification results and for a more standardised classification. The proposed procedure can be used as a model for fusing high spatial resolution multispectral imagery and lidar data for assessing forest attributes at the tree level. In addition, this fusion procedure has the potential to minimise human interaction in the interpretation of forest attributes.

## ACKNOWLEDGEMENT

This work was supported by the Australian Research Council (ARC) under Discovery Project DP0450889. The Ultracam-D data set was provided by IFMS Germany (<http://www.arcforest.com/>).

## REFERENCES

- Baltsavias, E.P.(1999) A comparison between photogrammetry and laser scanning, *ISPRS Journal of Photogrammetry and Remote Sensing*, Vol. 54, p. 83–94.
- Beucher, S. and Lantuejoul, C.(1979) Use of watersheds in contour detection, *Proceedings of International Workshop on Image Processing, Real-time Edge and Motion Detection/Estimation*, Rennes, France.
- Chen, Q., Balddochi, D., Gong, P. and Maggi, K.(2006) Isolating individual trees in a Savanna Woodland using small footprint lidar data, *Photogrammetric Engineering & Remote Sensing*, Vol. 72, No. 8, pp. 923-932.
- Clark, D.B., Castro, C.S., Alvarado, L.D.A. and Read, J.M.(2004) Quantifying mortality of tropical rain forest trees using high-spatial-resolution satellite data, *Ecological Letters*, Vol. 7, pp. 52-59.
- Gong, P., Biging, G.S., Lee, S.M., Mei, X., Sheng, Y., Pu, R., Xu, B., Schwarz, K. and Mostafa, M.(1999) Photo eometrics for forest inventory, *Geographic Information Science*, Vol. 5, pp. 9-14.
- Kalayeh, H.W. and Landgrebe, D.A.(1983) Predicting the required number of training samples, *IEEE Transactions on Pattern Analysis and Machine Intelligence*, Vol. 5, pp. 493-504.
- Kelly, M., Shaari, D., Guo, Q.H. and Liu, D.S(2004) A comparison of standard and hybrid classifier methods for mapping hardwood mortality in areas affected by "sudden oak death", *Photogrammetric Engineering & Remote Sensing*, Vol. 70, pp. 122-1239.
- Leberl, F. and Gruber, M.(2005) Ultracam-d: understanding some noteworthy capabilities, *Proceedings of Photogrammetric Week 2005*, Stuttgart, Germany.
- Leckie, D., Gougeon, F., Hill, D., Quinn, R., Armstrong, L. and Shreenan, R.(2003) Combinedhigh density LiDAR and multispectral imagery for individual tree crown analysis, *Canadian Journal of Remote Sensing*, Vol. 29, No. 5, p. 633–649.
- Meyer, F. and Beucher, S.(1990) Morphological segmentation, *Journal of Visual Communication and Image Representation*, Vol. 1, No. 1, pp. 21-46.
- Soille, P.(2003) *Morphological image analysis: principles and applications* (2nd Edition), Springer, Berlin ; New York. 316 pp.
- Sua'reza, J.C., Ontiveros, C., Smith, S. and Snape, S.(2005) Use of airborne LiDAR andaerial photography in the estimation of individual tree heights in forestry, *Computers & Geosciences* (2005), Vol. 31, No. 2, p. 253–262.



APPENDIX A. Tree Species Map of Moira state forest, nsw